applied sciences

MDPI

Article

Simple and Robust Log-Likelihood Ratio Calculation of Coded MPSK Signals in Wireless Sensor Networks for Healthcare

Bo Xie [1], Congfang Ma [2], Haiqiong Li [2], Gaoyuan Zhang [2,3,*] and Congzheng Han [3,*]

[1] School of Management, Henan University of Science and Technology, Luoyang 471023, China; boxie@haust.edu.cn
[2] School of Information Engineering, Henan University of Science and Technology, Luoyang 471023, China; mcf1272388148@163.com (C.M.); lihaiqiong96@163.com (H.L.)
[3] Key Laboratory of Middle Atmosphere and Global Environment Observation, Institute of Atmospheric Physics, Chinese Academy of Sciences, Beijing 100029, China
* Correspondence: zhanggaoyuan407@163.com (G.Z.); c.han@mail.iap.ac.cn (C.H.)

Abstract: The simple and robust log-likelihood ratio (LLR) computation of coded Multiple Phase Shift Keying (MPSK) signals in Wireless Sensor Networks (WSNs) is considered under both phase noncoherent and Rayleigh fading channels for healthcare applications. We first simplify the optimal LLR for phase noncoherent channel, the estimation of the instantaneous channel state information (CSI) for both the fading amplitude and the additive white Gaussian noise (AWGN) is successfully avoided, and the complexity-intensive process for zero-order Bessel function of the first kind is also perfectly eliminated. Furthermore, we also develop the simplified LLR under Rayleigh fading channel. Correspondingly, the variance estimation for both AWGN and the statistical characteristic of the fading amplitude is no longer required, and the complicated process for implementation of the exponential function is also successfully avoided. Compared to the calculation of optimal LLR with full complexity, the proposed method is implementation-friendly, which is practically desired for energy-limited WSNs. The simulations are developed in the context of low-density parity-check (LDPC) codes, and the corresponding results show that the detection performance is extremely close to that of the full-complexity LLR metrics. That is, the performance degradation is efficiently prevented, whereas complexity reduction is also successfully achieved.

Keywords: IEEE 802.15.4c; coded multiple phase shift keying; noncoherent detection; channel state information

Citation: Xie, B.; Ma, C.; Li, H.; Zhang, G.; Han, C. Simple and Robust Log-Likelihood Ratio Calculation of Coded MPSK Signals in Wireless Sensor Networks for Healthcare. *Appl. Sci.* **2022**, *12*, 2330. https://doi.org/10.3390/app12052330

Academic Editors: Hacene Fouchal and Alvaro Araujo Pinto

Received: 12 January 2022
Accepted: 18 February 2022
Published: 23 February 2022

1. Introduction

The rapid development of modern information and communication technologies, such as the Internet of Things, wireless communication, and cloud [1–5], makes remote healthcare, or tele-healthcare, simpler than before, as shown in Figure 1. In recent years, wireless sensor networks (WSNs) have matured to be used to improve quality of life, which is regarded as one of the key research fields in the healthcare application industry and has attracted more and more attention [6–13]. It is well known that, sensor nodes in WSNs generally adopt small embedded devices such as some wearable devices, and the battery power carried by a single node is limited. In the complex medical information environment, the application of WSNs is usually oriented to some large-scale monitoring fields, which is necessary to collect massive amounts of monitoring data. In order to realize the effective data acquisition of WSNs, it is very important to reduce the energy consumption of nodes. Multiple Phase Shift keying (MPSK) is provided in IEEE 802.15.4c standard [14,15]. Detection of coded MPSK signal has important research and application value by improving transmission efficiency, reducing the energy consumption of node transmission and improving the life cycle of healthcare network.

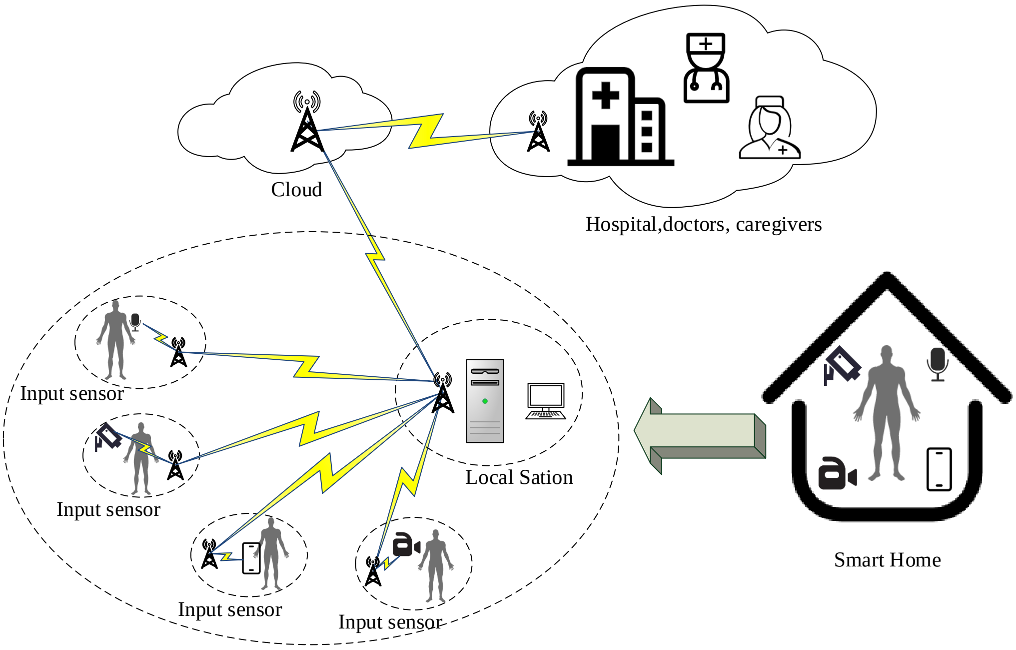

Figure 1. Wireless smart framework for transmission of home healthcare information.

In the literature, much progress has been achieved regarding the detection of coded MPSK signals. The work in [16] proposes a simplified soft decision metric for MPSK without the noise variance knowledge, and no performance loss is observed. In [17], the iterative decoding of LDPC coded MPSK is considered over time correlated Rayleigh fading channels. However, this research is developed under a coherent channel, which is clearly not suitable for our purposes. Under a phase noncoherent channel, the pilot-aided LLR for LDPC coded MPSK orthogonal frequency division multiplexing transmission is developed in [18]. However, it cannot be directly tailored for WSNs, wherein much attention is paid to low complexity, low cost, low power consumption. It is notable that much focus on the detection of uncoded binary phase shift keying (BPSK) signals in IEEE 802.15.4 WSNs has been witnessed in recent years [19–23]. Multiple-symbol detection (MSD) scheme for offset quadrature phase shift keying (O-QPSK) receivers is also considered in [24–27]. However, all of these are developed without channel coding.

In this work, we propose simple bit LLR calculation schemes for coded MPSK signals. Unlike the traditional noncoherent detection scheme which was equipped with an LLR extraction scheme with high complexity to achieve the best possible reliability, we pay all of our attention towards the simple design to balance complexity and reliability. We summarize our main contributions as follows.

- As a benchmark, the optimal bit LLR under a phase noncoherent channel is first given. For this scheme, both zero-order Bessel function and perfect instantaneous fading amplitude is involved. Thus, we propose a simple calculation configuration without CSI, which greatly simplifies the optimal scheme.
- The optimal bit LLR under a Rayleigh fading channel is also given, wherein we assume that the statistical characteristic of the fading amplitude is available. In this context, the variance estimation for both additive white Gaussian noise (AWGN) and the statistical characteristic of the fading amplitude is involved, and extensive exponential operation is also unavoidable. A simple calculation scheme is then developed.
- We find that the decision statistic is exactly the same under both phase noncoherent channels and the Rayleigh fading channel when no coding is considered, and no contribution from the fade amplitude and the variance of the AWGN noise is observed in this decision statistic. We also find that the CSI can be perfectly avoided in the bit

LLR calculation when channel coding is considered if the approximation is ingeniously designed and implemented to the optimal LLR.
- In order to verify the desirable properties of our proposed simple schemes, the characteristics of the receiver are studied from many aspects with extensive simulations.

We organize the rest of this paper as follows. Section 2 focuses on the system model under the fading channel. Section 3 introduces the LLR calculation under the phase noncoherent channel. In this case, the instantaneous fading amplitude is assumed to be available and known exactly at the receiver. Further relaxing this restriction, Section 4 concentrates on LLR calculation when the statistical characteristic for the fading amplitude is available at the receiver. The simulation results are discussed in Section 5. Finally, some conclusions and future work are provided in Section 6.

2. System Mode

Consider the transmission system depicted in Figure 2. The bit sequence $\boldsymbol{a}$ is encoded to generate the coded sequence $\boldsymbol{c}$. After interleaving, every four bits from $\boldsymbol{d}$ are finally mapped into a 16-bit chip sequence $\boldsymbol{S}$. Here, the modulation scheme is MPSK, and the Rayleigh fading channel is considered. Specifically, within N symbol intervals, the complex baseband received chip sequence $\boldsymbol{R}$ can be given as follows:

$$\boldsymbol{R} = (\boldsymbol{r}_1,\ \boldsymbol{r}_2,\ \cdots,\ \boldsymbol{r}_N), \tag{1}$$

where $\boldsymbol{r}_k = (r_{k,1},\ r_{k,2},\ \cdots,\ r_{k,16})$ and $1 \le k \le N$. Here, $r_{k,i} = \rho_{k,i} s_{y,i} e^{j\theta_{k,i}} + \eta_{k,i}$ and $1 \le i \le 16$. $\{s_{y,i}, 1 \le i \le 16\}$ represents the spreading sequence $\boldsymbol{s}_y$, which are selected from $\Lambda = \{\boldsymbol{s}_y, 1 \le y \le 16\}$ as depicted in Table 1. $\rho_{k,i}$ and $\theta_{k,i}$ denote the fading amplitude and phase, respectively. $\eta_{k,i}$ is a discrete, cyclic symmetric, complex Gaussian random process with zero mean and variance σ^2.

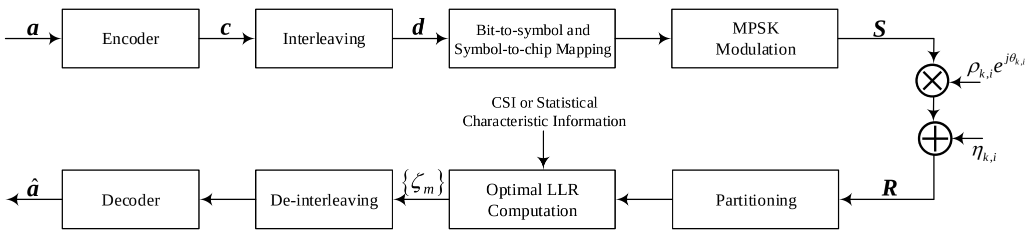

Figure 2. Traditional optimal noncoherent detection of coded MPSK in WSNs. $\rho_{k,i}$ is the fading amplitude, $\theta_{k,i}$ is the fading phase, and $\eta_{k,i}$ denotes the complex AWGN.

We assume that the fading amplitude $\rho_{k,i}$ and phase $\theta_{k,i}$ are unknown and random at the receiver, but are constant for some specified time period [19]. In other words, we make a piecewise constant approximation to these parameters, which is $\rho_{k,i} = \rho$, and $\theta_{k,i} = \theta$. In addition, ρ follows the Rayleigh distribution, and θ is uniformly distributed in the interval $(-\pi, \pi)$.

Table 1. Symbol-to-chip mapping for MPSK.

Spreading Sequence s_y	$b_m, 0 \le m \le 3$	Chip Phases for $\mathbf{s}_y = (s_{y,1}, s_{y,2}, \ldots, s_{y,15}, s_{y,16})$
$\mathbf{s}_1$	0000	$0, \frac{\pi}{16}, \frac{\pi}{4}, \frac{9\pi}{16}, \pi, -\frac{7\pi}{16}, \frac{\pi}{4}, -\frac{15\pi}{16}, 0, -\frac{15\pi}{16}, \frac{\pi}{4}, -\frac{7\pi}{16}, \pi, \frac{9\pi}{16}, \frac{\pi}{4}, \frac{\pi}{16}$
$\mathbf{s}_2$	1000	$\frac{\pi}{16}, 0, \frac{\pi}{16}, \frac{\pi}{4}, \frac{9\pi}{16}, \pi, -\frac{7\pi}{16}, \frac{\pi}{4}, -\frac{15\pi}{16}, 0, -\frac{15\pi}{16}, \frac{\pi}{4}, -\frac{7\pi}{16}, \pi, \frac{9\pi}{16}, \frac{\pi}{4}$
$\mathbf{s}_3$	0100	$\frac{\pi}{4}, \frac{\pi}{16}, 0, \frac{\pi}{16}, \frac{\pi}{4}, \frac{9\pi}{16}, \pi, -\frac{7\pi}{16}, \frac{\pi}{4}, -\frac{15\pi}{16}, 0, -\frac{15\pi}{16}, \frac{\pi}{4}, -\frac{7\pi}{16}, \pi, \frac{9\pi}{16}$
$\mathbf{s}_4$	1100	$\frac{9\pi}{16}, \frac{\pi}{4}, \frac{\pi}{16}, 0, \frac{\pi}{16}, \frac{\pi}{4}, \frac{9\pi}{16}, \pi, -\frac{7\pi}{16}, \frac{\pi}{4}, -\frac{15\pi}{16}, 0, -\frac{15\pi}{16}, \frac{\pi}{4}, -\frac{7\pi}{16}, \pi$
$\mathbf{s}_5$	0010	$\pi, \frac{9\pi}{16}, \frac{\pi}{4}, \frac{\pi}{16}, 0, \frac{\pi}{16}, \frac{\pi}{4}, \frac{9\pi}{16}, \pi, -\frac{7\pi}{16}, \frac{\pi}{4}, -\frac{15\pi}{16}, 0, -\frac{15\pi}{16}, \frac{\pi}{4}, -\frac{7\pi}{16}$
$\mathbf{s}_6$	1010	$-\frac{7\pi}{16}, \pi, \frac{9\pi}{16}, \frac{\pi}{4}, \frac{\pi}{16}, 0, \frac{\pi}{16}, \frac{\pi}{4}, \frac{9\pi}{16}, \pi, -\frac{7\pi}{16}, \frac{\pi}{4}, -\frac{15\pi}{16}, 0, -\frac{15\pi}{16}, \frac{\pi}{4}$
$\mathbf{s}_7$	0110	$\frac{\pi}{4}, -\frac{7\pi}{16}, \pi, \frac{9\pi}{16}, \frac{\pi}{4}, \frac{\pi}{16}, 0, \frac{\pi}{16}, \frac{\pi}{4}, \frac{9\pi}{16}, \pi, -\frac{7\pi}{16}, \frac{\pi}{4}, -\frac{15\pi}{16}, 0, -\frac{15\pi}{16}$
$\mathbf{s}_8$	1110	$-\frac{15\pi}{16}, \frac{\pi}{4}, -\frac{7\pi}{16}, \pi, \frac{9\pi}{16}, \frac{\pi}{4}, \frac{\pi}{16}, 0, \frac{\pi}{16}, \frac{\pi}{4}, \frac{9\pi}{16}, \pi, -\frac{7\pi}{16}, \frac{\pi}{4}, -\frac{15\pi}{16}, 0$
$\mathbf{s}_9$	0001	$0, -\frac{15\pi}{16}, \frac{\pi}{4}, -\frac{7\pi}{16}, \pi, \frac{9\pi}{16}, \frac{\pi}{4}, \frac{\pi}{16}, 0, \frac{\pi}{16}, \frac{\pi}{4}, \frac{9\pi}{16}, \pi, -\frac{7\pi}{16}, \frac{\pi}{4}, -\frac{15\pi}{16}$
$\mathbf{s}_{10}$	1001	$-\frac{15\pi}{16}, 0, -\frac{15\pi}{16}, \frac{\pi}{4}, -\frac{7\pi}{16}, \pi, \frac{9\pi}{16}, \frac{\pi}{4}, \frac{\pi}{16}, 0, \frac{\pi}{16}, \frac{\pi}{4}, \frac{9\pi}{16}, \pi, -\frac{7\pi}{16}, \frac{\pi}{4}$
$\mathbf{s}_{11}$	0101	$\frac{\pi}{4}, -\frac{15\pi}{16}, 0, -\frac{15\pi}{16}, \frac{\pi}{4}, -\frac{7\pi}{16}, \pi, \frac{9\pi}{16}, \frac{\pi}{4}, \frac{\pi}{16}, 0, \frac{\pi}{16}, \frac{\pi}{4}, \frac{9\pi}{16}, \pi, -\frac{7\pi}{16}$
$\mathbf{s}_{12}$	1101	$-\frac{7\pi}{16}, \frac{\pi}{4}, -\frac{15\pi}{16}, 0, -\frac{15\pi}{16}, \frac{\pi}{4}, -\frac{7\pi}{16}, \pi, \frac{9\pi}{16}, \frac{\pi}{4}, \frac{\pi}{16}, 0, \frac{\pi}{16}, \frac{\pi}{4}, \frac{9\pi}{16}, \pi$
$\mathbf{s}_{13}$	0011	$\pi, -\frac{7\pi}{16}, \frac{\pi}{4}, -\frac{15\pi}{16}, 0, -\frac{15\pi}{16}, \frac{\pi}{4}, -\frac{7\pi}{16}, \pi, \frac{9\pi}{16}, \frac{\pi}{4}, \frac{\pi}{16}, 0, \frac{\pi}{16}, \frac{\pi}{4}, \frac{9\pi}{16}$
$\mathbf{s}_{14}$	1011	$\frac{9\pi}{16}, \pi, -\frac{7\pi}{16}, \frac{\pi}{4}, -\frac{15\pi}{16}, 0, -\frac{15\pi}{16}, \frac{\pi}{4}, -\frac{7\pi}{16}, \pi, \frac{9\pi}{16}, \frac{\pi}{4}, \frac{\pi}{16}, 0, \frac{\pi}{16}, \frac{\pi}{4}$
$\mathbf{s}_{15}$	0111	$\frac{\pi}{4}, \frac{9\pi}{16}, \pi, -\frac{7\pi}{16}, \frac{\pi}{4}, -\frac{15\pi}{16}, 0, -\frac{15\pi}{16}, \frac{\pi}{4}, -\frac{7\pi}{16}, \pi, \frac{9\pi}{16}, \frac{\pi}{4}, \frac{\pi}{16}, 0, \frac{\pi}{16}$
$\mathbf{s}_{16}$	1111	$\frac{\pi}{16}, \frac{\pi}{4}, \frac{9\pi}{16}, \pi, -\frac{7\pi}{16}, \frac{\pi}{4}, -\frac{15\pi}{16}, 0, -\frac{15\pi}{16}, \frac{\pi}{4}, -\frac{7\pi}{16}, \pi, \frac{9\pi}{16}, \frac{\pi}{4}, \frac{\pi}{16}, 0$

3. LLR Calculation under Phase Noncoherent Channel

Assume that the fading phase is not known at the receiver, and the statistical average of this random phase is considered to eliminate the impact on our detection. Before launching the LLR calculation for decoding, it is instructive to point out the detection when no coding is considered. In this context, only the likelihood probability is required where the ith received chip sample of the kth symbol period is given by

$$r_{k,i} = \rho s_{y,i} e^{j\theta} + \eta_{k,i}. \tag{2}$$

Then, the likelihood probability in N symbol periods can be expressed as [28]:

$$p(\boldsymbol{R}|\boldsymbol{S},\theta) = \prod_{k=1}^{N}\prod_{i=1}^{16} p\left(r_{k,i}|s_{y,i},\theta\right) = \frac{1}{\left(\sqrt{2\pi}\sigma\right)^{16N}} \exp\left(-\frac{\| \boldsymbol{R} - \rho \boldsymbol{S} e^{j\theta} \|^2}{2\sigma^2}\right),\ 1 \le y \le 16 \tag{3}$$

where

$$\| \boldsymbol{R} - \rho \boldsymbol{S} e^{j\theta} \|^2 = \sum_{k=1}^{N}\sum_{i=1}^{16} \left| r_{k,i} - \rho s_{y,i} e^{j\theta} \right|^2 \tag{4}$$

After a simple analysis, we can express (4) in a more detailed form as follows [28]:

$$\begin{aligned}
\| \boldsymbol{R} - \rho \boldsymbol{S} e^{j\theta} \|^2 &= \| \boldsymbol{R} \|^2 + \rho^2 \| \boldsymbol{S} \|^2 - 2\rho \mathrm{Re}\left\{ \boldsymbol{R}^T \boldsymbol{S}^* \right\} e^{j(\theta-\beta)} \\
&= \sum_{k=1}^{N}\sum_{i=1}^{16} \left[\left| r_{k,i} \right|^2 + \rho^2 \left| s_{y,i} \right|^2 \right] - 2\rho \mathrm{Re}\left\{ \sum_{k=1}^{N}\sum_{i=1}^{16} r_{k,i} s_{y,i}^* \right\} \cos\theta \\
&\quad - 2\rho \mathrm{Im}\left\{ \sum_{k=1}^{N}\sum_{i=1}^{16} r_{k,i} s_{y,i}^* \right\} \sin\theta \\
&= \sum_{k=1}^{N}\sum_{i=1}^{16} \left[\left| r_{k,i} \right|^2 + \rho^2 \left| s_{y,i} \right|^2 \right] - 2\rho \left| \sum_{k=1}^{N}\sum_{i=1}^{16} r_{k,i} s_{y,i}^* \right| \cos(\theta - \beta)
\end{aligned} \tag{5}$$

where

$$\beta = \tan^{-1}\frac{\mathrm{Im}\{\boldsymbol{R}^T\boldsymbol{S}^*\}}{\mathrm{Re}\{\boldsymbol{R}^T\boldsymbol{S}^*\}} \tag{6}$$

As θ is assumed to be uniformly distributed, then the probability density function of $\boldsymbol{R}$ given the transmitted symbol sequence $\boldsymbol{S}$ can be given as

$$\begin{aligned} p(\boldsymbol{R}|\boldsymbol{S}) &= \int_{-\pi}^{\pi} p(\boldsymbol{R}|\boldsymbol{S},\theta)p(\theta)d\theta \\ &= \frac{1}{\left(\sqrt{2\pi}\sigma\right)^{16N}}\exp\left[-\frac{1}{2\sigma^2}\sum_{k=1}^{N}\sum_{i=1}^{16}\left[\left|r_{k,i}\right|^2+\rho^2\left|s_{y,i}\right|^2\right]\right] I_0\left(\frac{\rho}{\sigma^2}\left|\sum_{k=1}^{N}\sum_{i=1}^{16} r_{k,i}s_{y,i}^*\right|\right) \\ &= \frac{1}{\left(\sqrt{2\pi}\sigma\right)^{16N}}\exp\left[-\frac{\langle \boldsymbol{R},\boldsymbol{R}^*\rangle}{2\sigma^2}\right]\exp\left[-\frac{\langle \boldsymbol{S},\boldsymbol{S}^*\rangle}{2\sigma^2}\rho^2\right] I_0\left(\frac{|\langle \boldsymbol{R},\boldsymbol{S}^*\rangle|}{\sigma^2}\rho\right) \\ &\sim I_0\left(\frac{|\langle \boldsymbol{R},\boldsymbol{S}^*\rangle|}{\sigma^2}\rho\right) \\ &\sim |\langle \boldsymbol{R},\boldsymbol{S}^*\rangle| \end{aligned} \tag{7}$$

where $I_0(\cdot)$ is the zeroth order modified Bessel function of the first kind, $*$ represents the conjugation operation, and $\langle\cdot,\cdot\rangle$ denotes the correlation operation.

As shown in (7), a decision metric in conjugate correlation form is achieved when no coding is considered. The amplitude information for the fading channel is not required at the receiver, although we assume that perfect acquisition of this instantaneous CSI is available. Furthermore, the CSI for the AWGN channel can also be avoided. This follows from the fact that no contribution from the fade amplitude ρ and the variance σ^2 is observed in the decision metric given in (7). Next, we will focus on the LLR calculation when coding is involved. Specifically, we consider (a) an AWGN channel with perfect CSI, i.e., perfect knowledge of the variance σ^2 is available at the receiver, and (b) an AWGN channel without CSI, i.e., no knowledge of the variance σ^2 is available. In the first case, we will develop the optimal LLR calculation with full complexity. Clearly, in the second case, we will be given a simplified LLR calculation form without CSI.

According to (7), the LLR can be expressed as [29]:

$$\begin{aligned} \zeta_m &= \ln\frac{p(c_m{=}0|\boldsymbol{R})}{p(c_m{=}1|\boldsymbol{R})} = \ln\frac{\sum\limits_{\boldsymbol{S}_y:c_m=0} p(\boldsymbol{R}|\boldsymbol{S})}{\sum\limits_{\boldsymbol{S}_y:c_m=1} p(\boldsymbol{R}|\boldsymbol{S})} \\ &= \ln\frac{\sum\limits_{\boldsymbol{S}_y:c_m=0} I_0\left(\frac{\rho}{\sigma^2}\left|\sum\limits_{k=1}^{N}\sum\limits_{i=1}^{16} r_{k,i}s_{y,i}^*\right|\right)}{\sum\limits_{\boldsymbol{S}_y:c_m=1} I_0\left(\frac{\rho}{\sigma^2}\left|\sum\limits_{k=1}^{N}\sum\limits_{i=1}^{16} r_{k,i}s_{y,i}^*\right|\right)} \\ &= \ln\frac{\sum\limits_{\boldsymbol{S}_y:c_m=0} I_0\left(\frac{\rho}{\sigma^2}|\langle \boldsymbol{R},\boldsymbol{S}^*\rangle|\right)}{\sum\limits_{\boldsymbol{S}_y:c_m=1} I_0\left(\frac{\rho}{\sigma^2}|\langle \boldsymbol{R},\boldsymbol{S}^*\rangle|\right)},\ m\in\{0,\ 1,\ \cdots,4N-1\} \end{aligned} \tag{8}$$

Here, we introduce a method for extracting the bit LLR under the fading channels with perfect CSI, and then soft decision decoding can be used to improve receiver performance. However, there are still shortcomings of this scheme. First, the zero-order Bessel function is involved, and the resource consumption (implementation complexity, storage space, energy consumption, and delay) is relatively large, especially when the observation interval N is large. Second, in order to obtain the bit LLR information, the receiver needs to accurately estimate the CSI. An inaccurate estimation of the CSI would cause a serious deterioration in the subsequent decoding. That is, robustness to CSI is insufficiency. Therefore, in the following, we further turn our attention towards developing a bit LLR extraction scheme under multiple observation intervals with low complexity and no CSI.

First, calculate the decision metric for each symbol:

$$V_{k,y} = \left| \sum_{i=1}^{16} r_{k,i} s_{y,i}^{*} \right|^2, \ 1 \le y \le 16, 1 \le k \le N \tag{9}$$

Secondly, the maximum and two submaximal metrics for each symbol are recorded as follows [30]:

$$V_{k,\hat{y}_1} = \max_{1 \le y \le 16} \left\{ V_{k,y} \right\}, \ 1 \le k \le N \tag{10}$$

$$V_{k,\hat{y}_2} = \max_{1 \le y \le 16, y \ne \hat{y}_1} \left\{ V_{k,y} \right\}, \ 1 \le k \le N \tag{11}$$

$$V_{k,\hat{y}_3} = \max_{1 \le y \le 16, y \ne \{\hat{y}_1, \hat{y}_2\}} \left\{ V_{k,y} \right\}, \ 1 \le k \le N \tag{12}$$

The LLR in (8) is finally simplified as

$$\zeta_m = \ln \frac{\sum\limits_{S_y : c_m = 0, l} I_0\left(\frac{\rho}{\sigma^2} \left| \sum\limits_{k=1}^{N} w_{k,\hat{y}_l} \right| \right)}{\sum\limits_{S_y : c_m = 1, l} I_0\left(\frac{\rho}{\sigma^2} \left| \sum\limits_{k=1}^{N} w_{k,\hat{y}_l} \right| \right)}, \ l \in \{1, \ 2, \ 3\}, \ m \in \{0, \ 1, \ \cdots, 4N-1\} \tag{13}$$

where $w_{k,\hat{y}_l} = \sum\limits_{i=1}^{16} r_{k,i} s_{\hat{y}_l,i}^{*}$, and $\hat{y}_l$ is given in (10) to (12).

As shown in (13), the calculation number for $I_0(x)$ is successfully reduced. However, the implementation for $I_0(x)$ is also complicated for the receiver in WSN. Consequently, we will focus our attention on the simplification of $I_0(x)$. As shown in Figure 3, $I_0(x)$ increases rapidly with the increase in x, and the main influence of $\sum\limits_{S_y} I_0\left(\frac{\rho}{\sigma^2} \left| \sum\limits_{k=1}^{N} w_{k,\hat{y}_l} \right| \right)$ can be determined by $I_0\left(\max\limits_{S_y} \left[\frac{\rho}{\sigma^2} \left| \sum\limits_{k=1}^{N} w_{k,\hat{y}_l} \right| \right] \right)$. Therefore, we can modify (13) as

$$\zeta_m \approx \ln \frac{I_0\left(\max\limits_{S_y : c_m = 0, l} \left[\frac{\rho}{\sigma^2} \left| \sum\limits_{k=1}^{N} w_{k,\hat{y}_l} \right| \right] \right)}{I_0\left(\max\limits_{S_y : c_m = 1, l} \left[\frac{\rho}{\sigma^2} \left| \sum\limits_{k=1}^{N} w_{k,\hat{y}_l} \right| \right] \right)} \tag{14}$$

Under low SNR, taking the first two items of Taylor series expansion for $I_0(\cdot)$ [31], (14) can be simplified as

$$\zeta_m \approx \ln \frac{1 + \frac{\rho^2}{4\sigma^4} \left[\max\limits_{S_y : c_m = 0, l} \left(\left| \sum\limits_{k=1}^{N} w_{k,\hat{y}_l} \right| \right) \right]^2}{1 + \frac{\rho^2}{4\sigma^4} \left[\max\limits_{S_y : c_m = 1, l} \left(\left| \sum\limits_{k=1}^{N} w_{k,\hat{y}_l} \right| \right) \right]^2} \tag{15}$$

Note that when $z \to 0$, $\ln(1+z) \approx z$, and $\ln \frac{(1+z_1)}{(1+z_2)} \approx z_1 - z_2$. Then, (15) can be further simplified to

$$\zeta_m \approx \frac{\rho^2}{4\sigma^4}\left\{\left[\max_{S_y:c_m=0,l}\left(\left|\sum_{k=1}^{N} w_{k,\hat{y}_l}\right|\right)\right]^2 - \left[\max_{S_y:c_m=1,l}\left(\left|\sum_{k=1}^{N} w_{k,\hat{y}_l}\right|\right)\right]^2\right\} \tag{16}$$

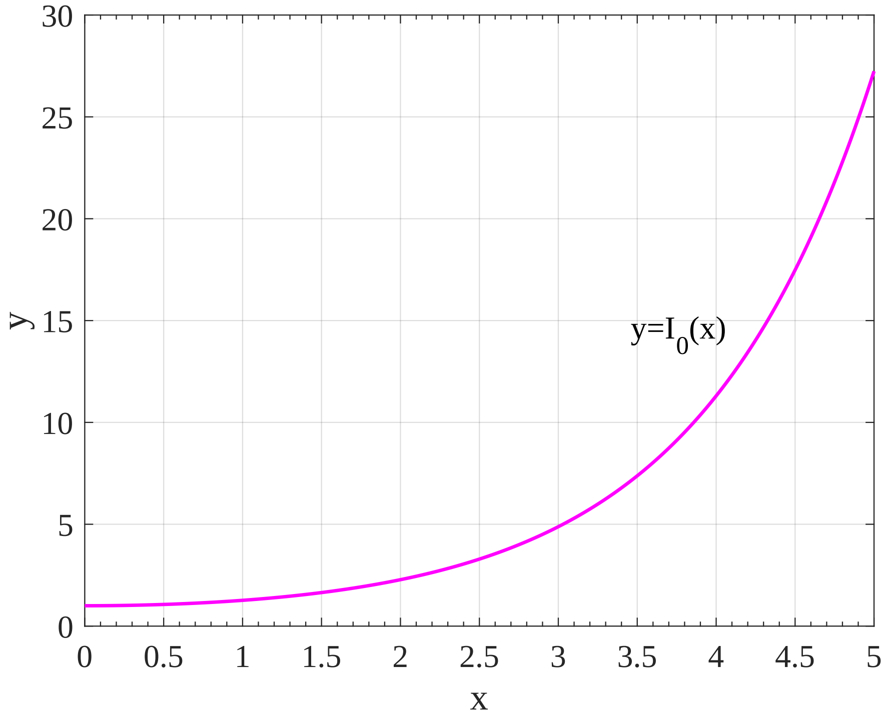

Figure 3. Bessel function I_0.

In (16), $\frac{\rho^2}{4\sigma^4}$ is a constant term. If the min-sum (MS) algorithm for LDPC code or the soft output Viterbi algorithm (SOVA) algorithm for the convolutional code is considered, removing $\frac{\rho^2}{4\sigma^4}$ will not affect the decoding result. Therefore, after eliminating $\frac{\rho^2}{4\sigma^4}$ in (16), the LLR can be given as follows:

$$\zeta_m \approx \left[\max_{S_y:c_m=0,l}\left(\left|\sum_{k=1}^{N} w_{k,\hat{y}_l}\right|\right)\right]^2 - \left[\max_{S_y:c_m=1,l}\left(\left|\sum_{k=1}^{N} w_{k,\hat{y}_l}\right|\right)\right]^2, \tag{17}$$

where $l \in \{1,2,3\}, m \in \{0,1,\cdots,4N-1\}$.

4. LLR Calculation under Rayleigh Fading Channel

As shown in Section 3, we assume that the instantaneous amplitude information for the fading channel is available, and a phase noncoherent channel is considered. In this section, we will relax this condition and assume that only the statistical characteristic for the fading amplitude is available. Note that the main problem for the receiver now becomes to how to exploit this statistical information, thereby optimizing the design and then coming up with a detection scheme. In this context, the statistical average is also considered to eliminate the impact on the detection, which is similar to the method we adopted in Section 3. In particular, the PDF of ρ is known as the Rayleigh distribution:

$$p(\rho) = \frac{\rho}{\sigma_\rho^2}\exp\left(-\frac{\rho^2}{2\sigma_\rho^2}\right), \rho \geq 0 \tag{18}$$

The likelihood function $p(\boldsymbol{R}|\boldsymbol{S})$ can be easily specialized as [28]

$$\begin{aligned} p(\boldsymbol{R}|\boldsymbol{S}) &= \int_0^\infty p(\boldsymbol{R}|\boldsymbol{S},\rho)p(\rho)d\rho \\ &= \int_0^\infty \frac{1}{(\sqrt{2\pi}\sigma)^{16N}} \exp\left[-\frac{1}{2\sigma^2}\sum_{k=1}^{N}\sum_{i=1}^{16}\left[\left|r_{k,i}\right|^2+\rho^2\left|s_{y,i}\right|^2\right]\right] I_0\left(\frac{\rho}{\sigma^2}\left|\sum_{k=1}^{N}\sum_{i=1}^{16} r_{k,i}s_{y,i}^*\right|\right)\frac{\rho}{\sigma_\rho^2}\exp\left[-\frac{\rho^2}{2\sigma_\rho^2}\right]d\rho \\ &= \frac{1}{\sigma_\rho^2(\sqrt{2\pi}\sigma)^{16N}}\exp\left[-\frac{\sum_{k=1}^{N}\sum_{i=1}^{16}|r_{k,i}|^2}{2\sigma^2}\right]\int_0^\infty \rho\exp\left[-\frac{\sigma_\rho^2\sum_{k=1}^{N}\sum_{i=1}^{16}\left|s_{y,i}\right|^2+\sigma^2}{2\sigma^2\sigma_\rho^2}\rho^2\right] I_0\left(\frac{\left|\sum_{k=1}^{N}\sum_{i=1}^{16} r_{k,i}s_{y,i}^*\right|}{\sigma^2}\rho\right)d\rho \\ &= \frac{1}{\sigma_\rho^2(\sqrt{2\pi}\sigma)^{16N}}\exp\left[-\frac{\langle \boldsymbol{R},\boldsymbol{R}^*\rangle}{2\sigma^2}\right]\int_0^\infty \rho\exp\left[-\frac{\sigma_\rho^2\langle \boldsymbol{S},\boldsymbol{S}^*\rangle+\sigma^2}{2\sigma^2\sigma_\rho^2}\rho^2\right] I_0\left(\frac{|\langle \boldsymbol{R},\boldsymbol{S}^*\rangle|}{\sigma^2}\rho\right)d\rho \end{aligned} \tag{19}$$

Note that statistical average is utilized in (19) to eliminate the randomness of the fade amplitude ρ. Furthermore, considering the following result [32]:

$$\int_0^\infty u\exp\left[-bu^2\right]I_0(cu)du = \frac{1}{2b}\exp\left(\frac{c^2}{4b}\right), \tag{20}$$

we can immediately develop the likelihood function $p(\boldsymbol{R}|\boldsymbol{S})$ in an explicit form as:

$$\begin{aligned} p(\boldsymbol{R}|\boldsymbol{S}) &= \frac{\sigma^2}{\left(\sqrt{2\pi}\sigma\right)^{16N}\left(\sigma_\rho^2\sum_{k=1}^{N}\sum_{i=1}^{16}\left|s_{y,i}\right|^2+\sigma^2\right)} \\ &\quad\times\exp\left[-\frac{\sum_{k=1}^{N}\sum_{i=1}^{16}\left|r_{k,i}\right|^2}{2\sigma^2}\right]\exp\left(\frac{\left|\sum_{k=1}^{N}\sum_{i=1}^{16} r_{k,i}s_{y,i}^*\right|^2\sigma_\rho^2}{2\sigma^2\left(\sigma_\rho^2\sum_{k=1}^{N}\sum_{i=1}^{16}\left|s_{y,i}\right|^2+\sigma^2\right)}\right) \\ &= \frac{\sigma^2}{\left(\sqrt{2\pi}\sigma\right)^{16N}\left(\sigma_\rho^2\langle \boldsymbol{S},\boldsymbol{S}^*\rangle+\sigma^2\right)}\exp\left[-\frac{\langle \boldsymbol{R},\boldsymbol{R}^*\rangle}{2\sigma^2}\right]\exp\left(\frac{|\langle \boldsymbol{R},\boldsymbol{S}^*\rangle|^2\sigma_\rho^2}{2\sigma^2\left(\sigma_\rho^2\langle \boldsymbol{S},\boldsymbol{S}^*\rangle+\sigma^2\right)}\right) \\ &\sim \exp\left(\frac{|\langle \boldsymbol{R},\boldsymbol{S}^*\rangle|^2\sigma_\rho^2}{2\sigma^2\left(\sigma_\rho^2\langle \boldsymbol{S},\boldsymbol{S}^*\rangle+\sigma^2\right)}\right) \\ &\sim |\langle \boldsymbol{R},\boldsymbol{S}^*\rangle|^2 \end{aligned} \tag{21}$$

The LLR can be then easily expressed as

$$\begin{aligned} \varsigma_m &= \ln\frac{p(c_m=0|\boldsymbol{R})}{p(c_m=1|\boldsymbol{R})} = \ln\frac{\sum_{\boldsymbol{S}_y:c_m=0} p(\boldsymbol{R}|\boldsymbol{S})}{\sum_{\boldsymbol{S}_y:c_m=1} p(\boldsymbol{R}|\boldsymbol{S})} = \ln\frac{\sum_{\boldsymbol{S}_y:c_m=0}\exp\left(\frac{\left|\sum_{k=1}^{N}\sum_{i=1}^{16} r_{k,i}s_{y,i}^*\right|^2\sigma_\rho^2}{2\sigma^2\left(\sigma_\rho^2\sum_{k=1}^{N}\sum_{i=1}^{16}\left|s_{y,i}\right|^2+\sigma^2\right)}\right)}{\sum_{\boldsymbol{S}_y:c_m=1}\exp\left(\frac{\left|\sum_{k=1}^{N}\sum_{i=1}^{16} r_{k,i}s_{y,i}^*\right|^2\sigma_\rho^2}{2\sigma^2\left(\sigma_\rho^2\sum_{k=1}^{N}\sum_{i=1}^{16}\left|s_{y,i}\right|^2+\sigma^2\right)}\right)} \\ &= \ln\frac{\sum_{\boldsymbol{S}_y:c_m=0}\exp\left(\frac{|\langle \boldsymbol{R},\boldsymbol{S}^*\rangle|^2\sigma_\rho^2}{2\sigma^2\left(\sigma_\rho^2\langle \boldsymbol{S},\boldsymbol{S}^*\rangle+\sigma^2\right)}\right)}{\sum_{\boldsymbol{S}_y:c_m=1}\exp\left(\frac{|\langle \boldsymbol{R},\boldsymbol{S}^*\rangle|^2\sigma_\rho^2}{2\sigma^2\left(\sigma_\rho^2\langle \boldsymbol{S},\boldsymbol{S}^*\rangle+\sigma^2\right)}\right)},\ m\in\{0,\ 1,\ \cdots,4N-1\} \end{aligned} \tag{22}$$

As shown in (22), the implementation process for the LLR is complicated, especially when the observation interval N is large. Using (10), (11), and (12), (22) can be simplified as:

$$\begin{aligned}\varsigma_m &\approx \ln \frac{\sum\limits_{S_y:c_m=0,l} \exp\left(\frac{\left|\sum\limits_{k=1}^{N} w_{k,\hat{y}_l}\right|^2 \sigma_\rho^2}{2\sigma^2\left(\sigma_\rho^2 \sum\limits_{k=1}^{N}\sum\limits_{i=1}^{16}\left|s_{y,i}\right|^2+\sigma^2\right)}\right)}{\sum\limits_{S_y:c_m=1,l} \exp\left(\frac{\left|\sum\limits_{k=1}^{N} w_{k,\hat{y}_l}\right|^2 \sigma_\rho^2}{2\sigma^2\left(\sigma_\rho^2 \sum\limits_{k=1}^{N}\sum\limits_{i=1}^{16}\left|s_{y,i}\right|^2+\sigma^2\right)}\right)} \\ &= \ln \frac{\sum\limits_{S_y:c_m=0,l} \exp\left(\frac{\left|\sum\limits_{k=1}^{N} w_{k,\hat{y}_l}\right|^2 \sigma_\rho^2}{2\sigma^2\left(\sigma_\rho^2\langle \mathbf{S},\mathbf{S}^*\rangle+\sigma^2\right)}\right)}{\sum\limits_{S_y:c_m=1,l} \exp\left(\frac{\left|\sum\limits_{k=1}^{N} w_{k,\hat{y}_l}\right|^2 \sigma_\rho^2}{2\sigma^2\left(\sigma_\rho^2\langle \mathbf{S},\mathbf{S}^*\rangle+\sigma^2\right)}\right)}, \ l \in \{1,\ 2,\ 3\},\ m \in \{0,\ 1,\ \cdots, 4N-1\}\end{aligned} \tag{23}$$

Obviously, the next task is how to simplify the exponential operation in (23). Directly following the fact that [33]

$$\begin{aligned}\ln[\exp(\delta_1)+\cdots+\exp(\delta_J)] &\approx \ln\{\max[\exp(\delta_1),\cdots,\exp(\delta_J)]\} \\ &= \max[\ln\exp(\delta_1),\cdots,\ln\exp(\delta_J)] \\ &= \max(\delta_1,\cdots,\delta_J),\end{aligned} \tag{24}$$

(23) can be further simplified as:

$$\begin{aligned}\varsigma_m &\approx \frac{\sigma_\rho^2}{2\sigma^2\left(\sigma_\rho^2 \sum\limits_{k=1}^{N}\sum\limits_{i=1}^{16}\left|s_{y,i}\right|^2+\sigma^2\right)}\left\{\max_{S_y:c_m=0,l}\left|\sum_{k=1}^{N} w_{k,\hat{y}_l}\right|^2 - \max_{S_y:c_m=1,l}\left|\sum_{k=1}^{N} w_{k,\hat{y}_l}\right|^2\right\} \\ &= \frac{\sigma_\rho^2}{2\sigma^2\left(\sigma_\rho^2\langle \mathbf{S},\mathbf{S}^*\rangle+\sigma^2\right)}\left\{\max_{S_y:c_m=0,l}\left|\sum_{k=1}^{N} w_{k,\hat{y}_l}\right|^2 - \max_{S_y:c_m=1,l}\left|\sum_{k=1}^{N} w_{k,\hat{y}_l}\right|^2\right\},\end{aligned} \tag{25}$$

where $l \in \{1,2,3\}, m \in \{0,1,\cdots,4N-1\}$.

After eliminating the constant term $\frac{\sigma_\rho^2}{2\sigma^2\left(\sigma_\rho^2 \sum_{k=1}^{N}\sum_{i=1}^{16}\left|s_{y,i}\right|^2+\sigma^2\right)}$ in (25), the LLR can be obtained:

$$\varsigma_m = \max_{S_y:c_m=0,l}\left|\sum_{k=1}^{N} w_{k,\hat{y}_l}\right|^2 - \max_{S_y:c_m=1,l}\left|\sum_{k=1}^{N} w_{k,\hat{y}_l}\right|^2, \ l \in \{1,\ 2,\ 3\},\ m \in \{0,\ 1,\ \cdots, 4N-1\} \tag{26}$$

Comparing (21) with (7), we find that when there is no coding, the decision statistics are $|\langle \boldsymbol{R}, \boldsymbol{S}\rangle|$ and $|\langle \boldsymbol{R}, \boldsymbol{S}\rangle|^2$ respectively, which are obviously equivalent. Therefore, the decision result is not affected by the fading multiplicative ρ without coding.

5. Numerical Results and Discussion

In this section, we analyze the performance of the proposed scheme from multiple dimensions by simulating the bit error rate (BER), symbol error rate (SER) and packet error rate (PER) performance, variance, and phase robustness of different schemes, as well as the complexity of the numerical calculation process. Note that in our simulation, the MPSK modulation is used, the (1008, 504) LDPC code shown in Figure 4 is considered, and the code rate is 0.5. The sum-product algorithm (SPA) or MS algorithm is considered for decoding [34], and the maximum number of iterations is set to 10. The detailed simulation parameters are shown in Table 2. For all the simulation results, we simulated enough symbols for each E_b/N_0 to collect at least 3000 symbol errors.

Table 2. Parameters used in simulations.

Parameter	Detailed Description
Channel condition	phase noncoherent or Rayleigh fading
Power of the complex AWGN	$1/SNR$
Timing synchronization	Perfect
LDPC code	PEGReg (1008, 504)
Code rate	0.5
Degree distribution	(3, 6)
Data modulation	MPSK
Symbols	16-ary orthogonal
Payload length of PPDU (bits)	504
Spreading factor	16
Chip rate (Mchip/s)	1
Symbol rate (ks/s)	62.5
Binary data rate (kb/s)	250
Carrier frequency (MHz)	786
fading phase θ (rads)	Uniform distribution in $(-\pi, \pi)$
PN length	16
fading amplitude ρ	Rayleigh distribution

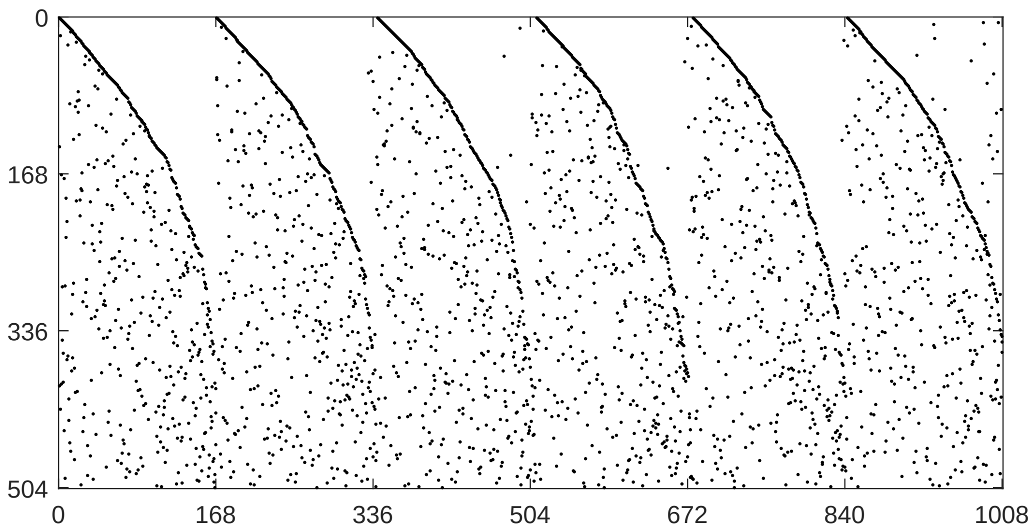

Figure 4. H matrix of (1008, 504) LDPC code.

5.1. The Influence of the Maximum Iteration Number on Detection Performance

In a phase noncoherent channel with different iteration numbers, the BER, SER, and PER performance of the exact LLR in (8) are shown in Figure 5, where $\rho = 1$, $N = 1$. It can be seen from Figure 5 that when the maximum number of iterations is increased from 1 to 25, the BER, SER, and PER performance can be improved under fading channels. In particular, as shown in Figure 5a, when BER = 1×10^{-5}, as the maximum number of iterations increases from one to three, the SNR gain is approximately 2 dB; when the maximum number of iterations is increased from three to five, the SNR gain is approximately 0.6 dB; when the maximum number of iterations is increased from five to eight, the SNR gain is approximately 0.3 dB; when the number of iterations is increased from eight to ten, the SNR gain is about 0.1 dB. Furthermore, after eight iterations, the performance can meet the requirement of the receiver. Additionally, the improvement is so small when the iteration ranges from 10 to 25 that we set the maximum number of iterations to be 10.

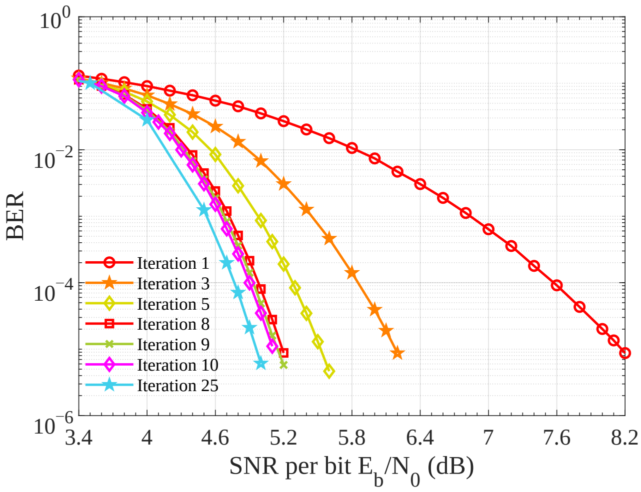

(**a**)

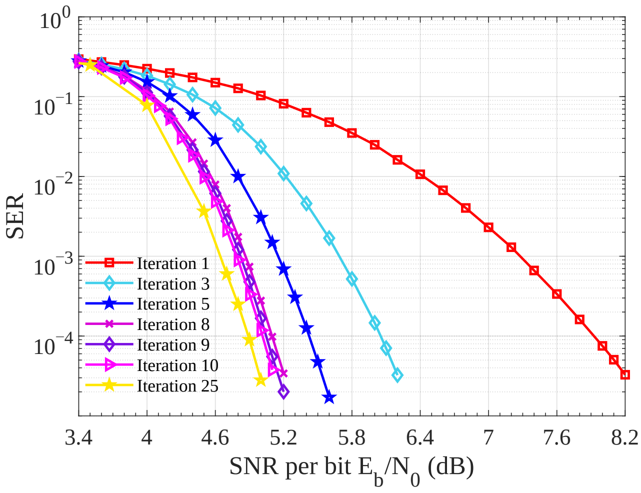

(**b**)

Figure 5. *Cont.*

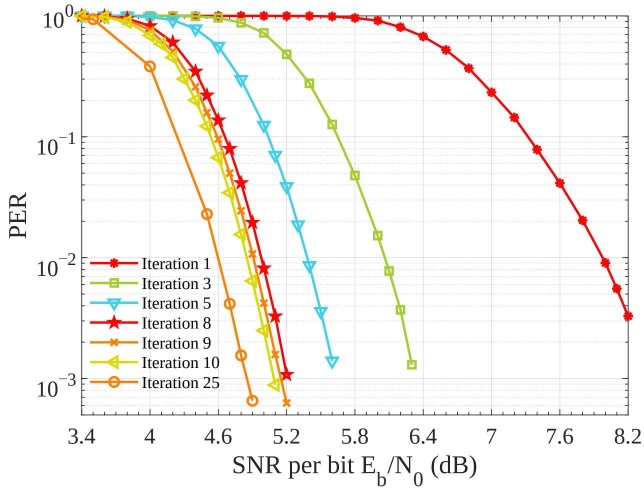

(**c**)

Figure 5. Under phase noncoherent channel with perfect CSI, the impact of the maximum number of iterations of the LDPC decoder on the detection performance, where $\rho = 1$. (**a**) BER performance; (**b**) SER performance; and (**c**) PER performance.

5.2. Detection Performance under Phase Noncoherent Channel

Under phase noncoherent channel, the BER, PER, and SER performance of the proposed simplified scheme, uncoded scheme, and the exact LLR scheme are verified, where $\rho = 1$, $N = 1$. As can be seen from Figure 6, compared with the uncoded scheme, the detection performance of the coding scheme is significantly improved. In addition, the performance of the simplified LLR scheme is extremely close to that of the exact LLR scheme. As shown in Figure 6c, when PER = 1×10^{-3}, compared with the uncoded scheme, the proposed simplified scheme obtains a gain of nearly 5.7 dB. Further, compared with the exact LLR scheme, the simplified LLR scheme in (13) only has a performance loss of about 0.04 dB, and the simplified LLR schemes in (16) and (17) has a performance loss of about 0.16 dB. Therefore, the simplified scheme has little performance loss and friendly-complexity. In particular, the simplified LLR scheme in (16) do not require CSI when using MS decoding. In addition, as shown in Figure 7, we can draw similar conclusions under $\rho \neq 1$, which however is not illustrated here. In a word, our simulation results in Figures 6 and 7 indicate that our simplified LLR scheme depicts good performance under the phase noncoherent channel. Note that no CSI and process for zero-order Bessel function of the first kind is needed in our simplified scheme.

5.3. Detection Performance under Rayleigh Fading Channel

In the Rayleigh fading channel, the BER, PER, and SER performance of the proposed simplified scheme, uncoded scheme, and the exact LLR scheme are verified. As can be seen from Figure 8, compared with the uncoded scheme, the detection performance of the coding scheme is significantly improved. The performance of the simplified LLR scheme is extremely close to that of the exact LLR scheme. As shown in Figure 8c, when PER = 1×10^{-3}, compared with the uncoded scheme, the proposed simplified scheme obtains a gain of nearly 6.1 dB. Compared with the exact LLR scheme, the simplified LLR scheme in (25) only has a performance loss of about 0.02 dB, and the simplified LLR scheme in (26) has a performance loss of about 0.1 dB. Therefore, the simplified scheme has little performance loss and friendly-complexity. In particular, the simplified LLR schemes in (26) do not require CSI when using MS decoding. In addition, as shown in Figure 9, we can draw similar conclusions under $\rho \neq 1$, which, however, is not illustrated here. Clearly, our simulation results in Figures 8 and 9 indicate that our simplified LLR scheme depicts good performance under the Rayleigh fading channel.

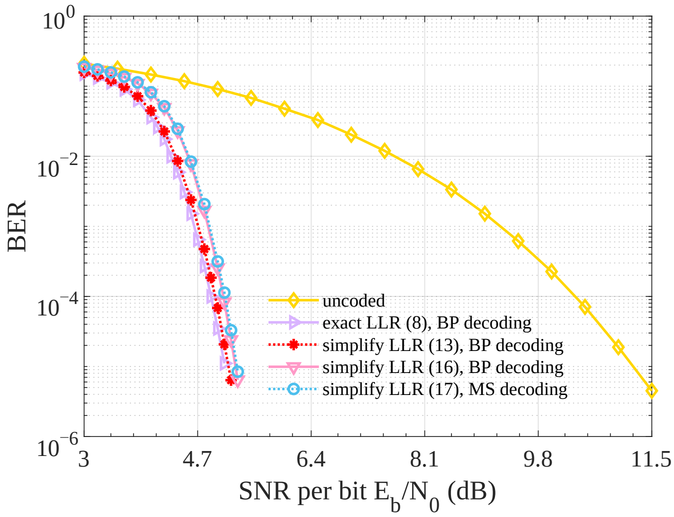

(**a**)

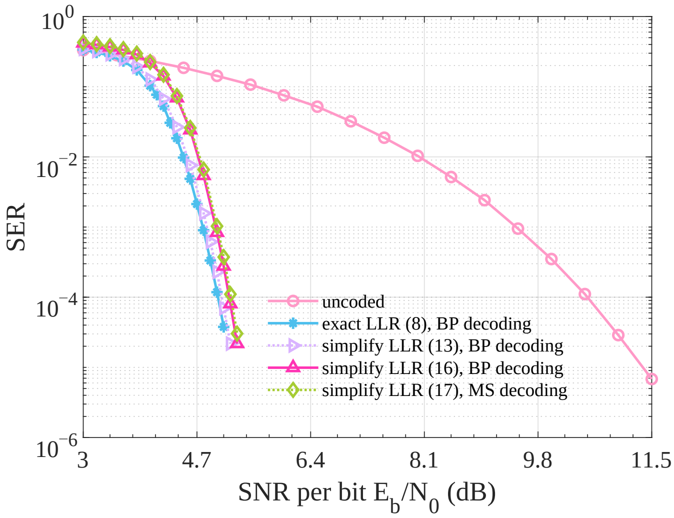

(**b**)

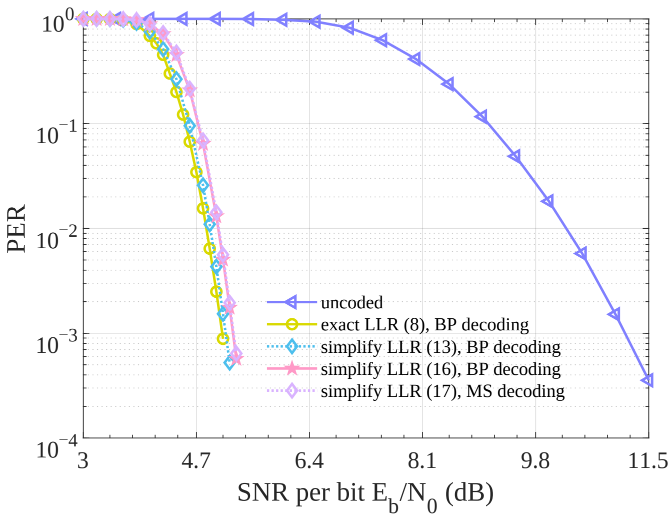

(**c**)

Figure 6. Detection performance for LDPC coded IEEE 802.15.4c MPSK signals under phase non-coherent channel, wherein different LLR calculation schemes are considered and $\rho = 1$. (**a**) BER performance; (**b**) SER performance; and (**c**) PER performance.

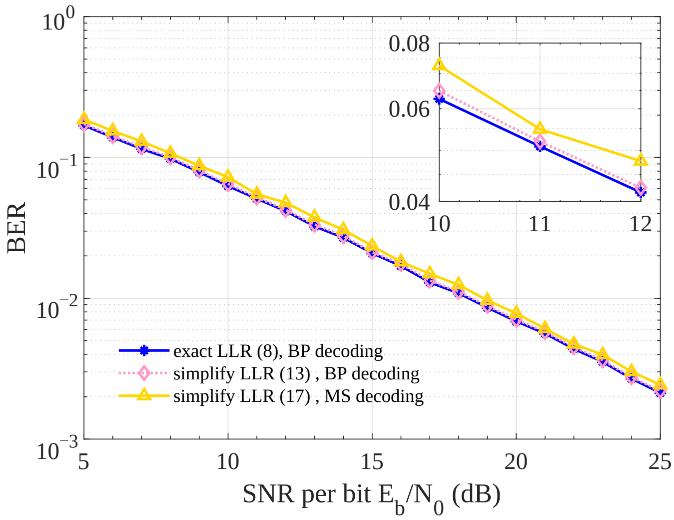

(**a**)

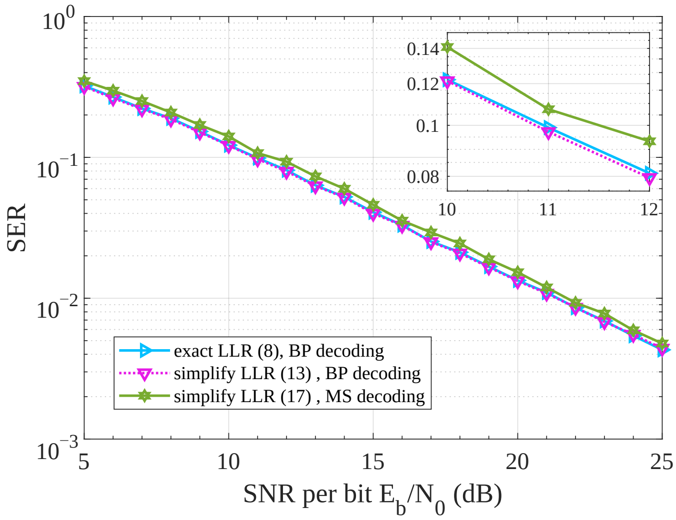

(**b**)

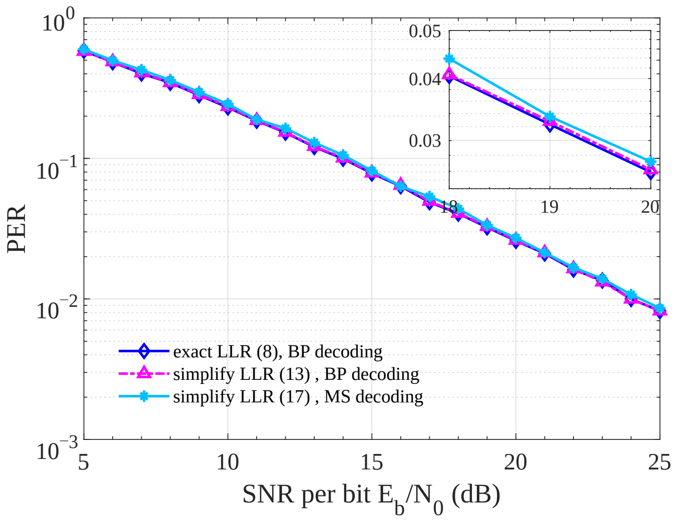

(**c**)

Figure 7. Detection performance for LDPC coded IEEE 802.15.4c MPSK signals under phase non-coherent channel, wherein different LLR calculation schemes are considered and $\rho \neq 1$. (**a**) BER performance; (**b**) SER performance; and (**c**) PER performance.

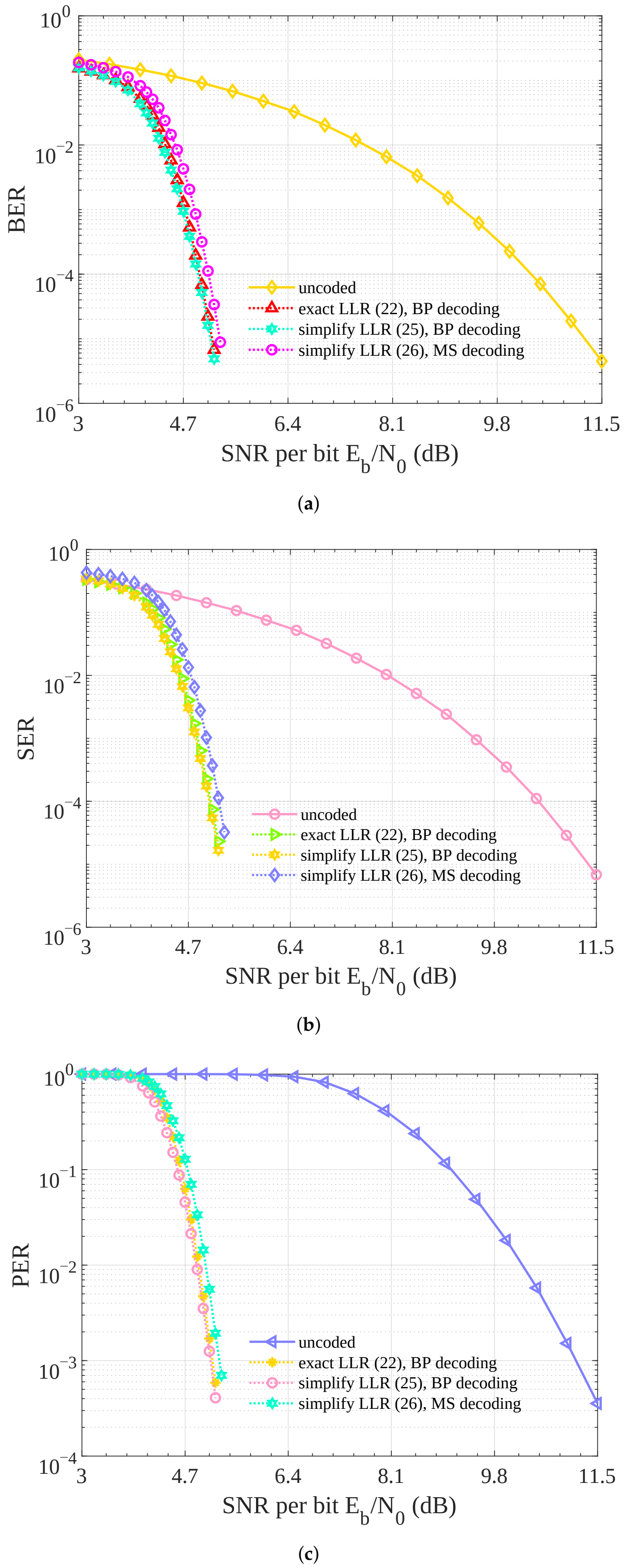

Figure 8. Detection performance for LDPC coded IEEE 802.15.4c MPSK signals under Rayleigh fading channel, wherein different LLR calculation schemes are considered and $\rho = 1$. (**a**) BER performance; (**b**) SER performance; and (**c**) PER performance.

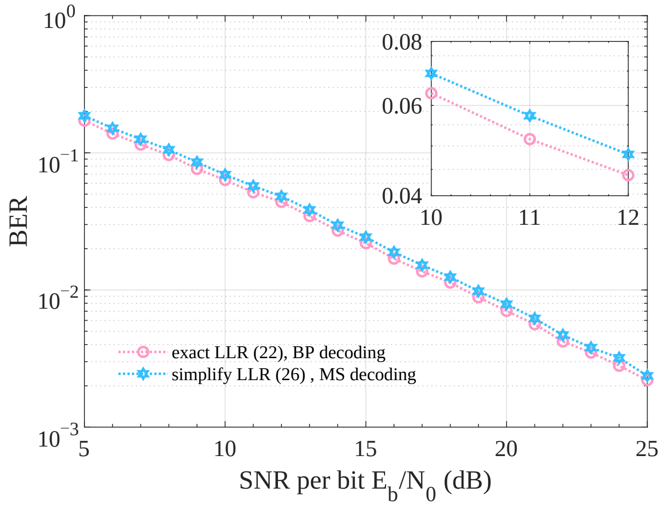

(**a**)

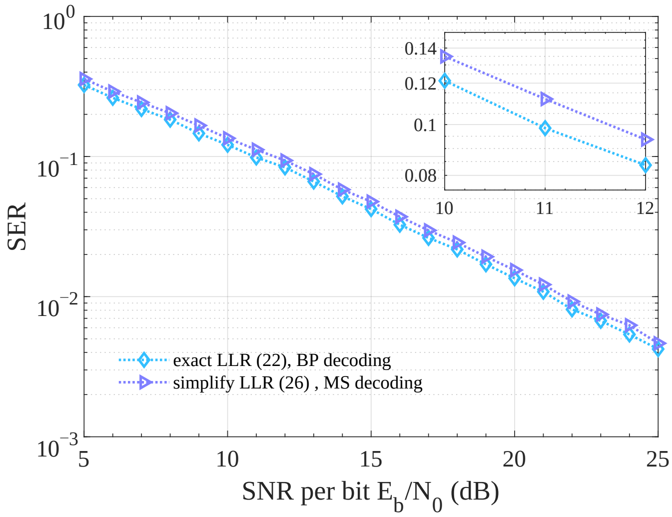

(**b**)

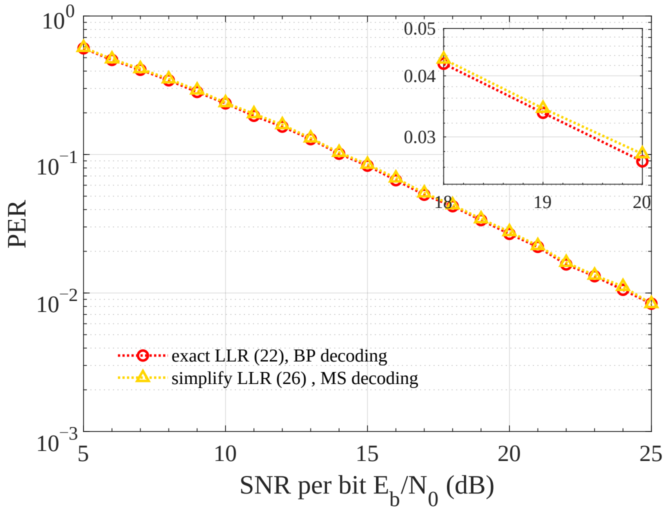

(**c**)

Figure 9. Detection performance for LDPC coded IEEE 802.15.4c MPSK signals under Rayleigh fading channel, wherein different LLR calculation schemes are considered and $\rho \neq 1$. (**a**) BER performance; (**b**) SER performance; and (**c**) PER performance.

5.4. Variance Robustness

Figures 10 and 11 show the performance of exact LLR given in (8) and (21) under different CSI estimation errors, where $\Delta\sigma^2 = \alpha\sigma^2$, and $\rho = 1$. It can be seen from Figures 10 and 11 that when the variance estimation error of the AWGN is large, the detection performance of the exact LLR scheme is seriously attenuated. It is caused by a large CSI estimation error. That is, the exact LLR scheme has poor robustness to CSI. However, our proposed the simplified LLR scheme using MS decoding does not need CSI, so it has better robustness.

5.5. CPO Robustness

In this part, we study the detection performance of the LLR schemes given in (8) and (16) in fading channel with changing carrier phase, where $\rho = 1$. The phase θ is modeled as a Wiener process, wherein its initial value is uniformly chosen from $(-\pi, \pi)$. As shown in Figures 12 and 13, the performance of the proposed receiver does not significantly degrade if we increase the standard deviation of jitter from 0 degrees to 7 degrees. In addition, an irreducible error floor is observed for the LLR given in (8) and (16) with the increase in SNR. As shown in Figure 13, our proposed LLR scheme in (16) is clearly robust to dynamic phase jitter.

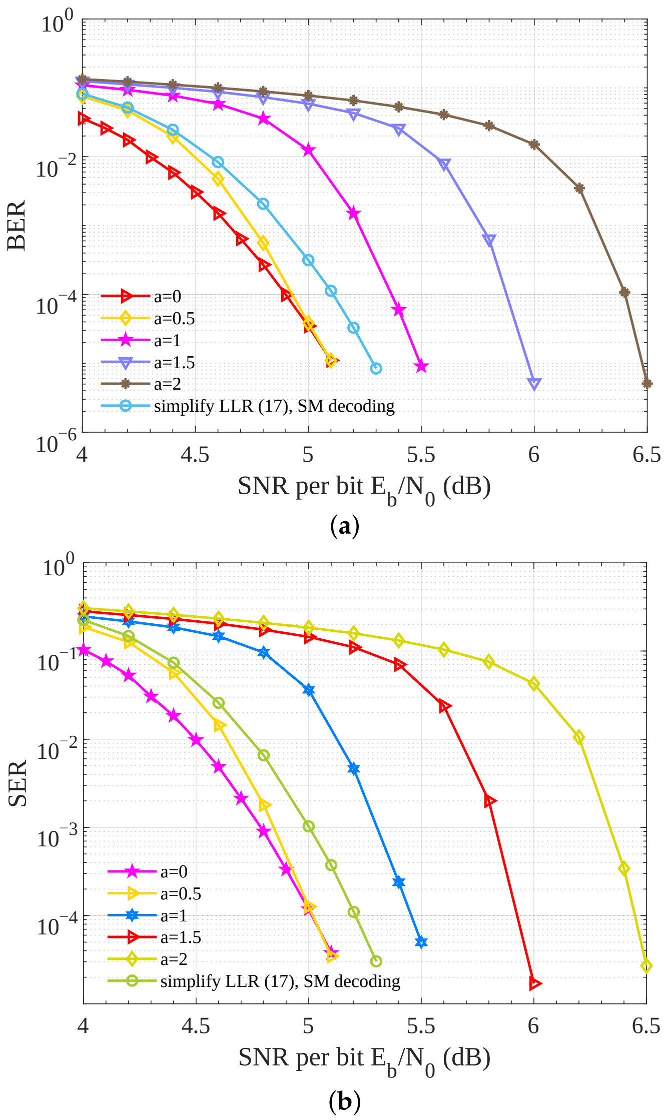

Figure 10. *Cont.*

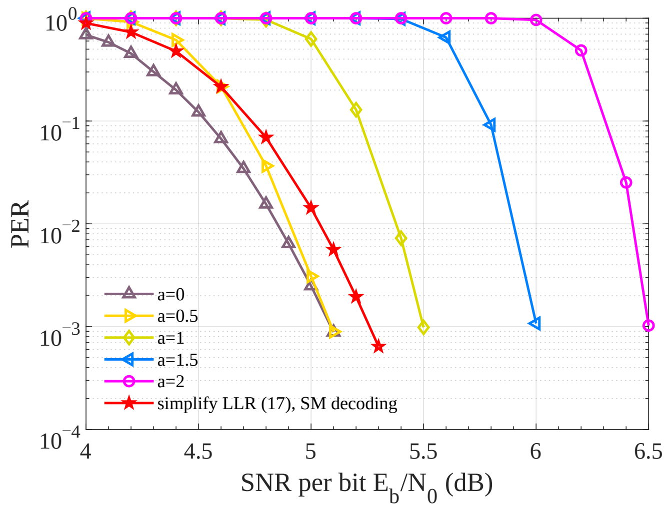

(**c**)

Figure 10. Detection performance for LDPC coded IEEE 802.15.4c MPSK signals under phase noncoherent channel with $\Delta\sigma^2 = \alpha\sigma^2$, where $\rho = 1$. (**a**) BER performance; (**b**) SER performance; and (**c**) PER performance.

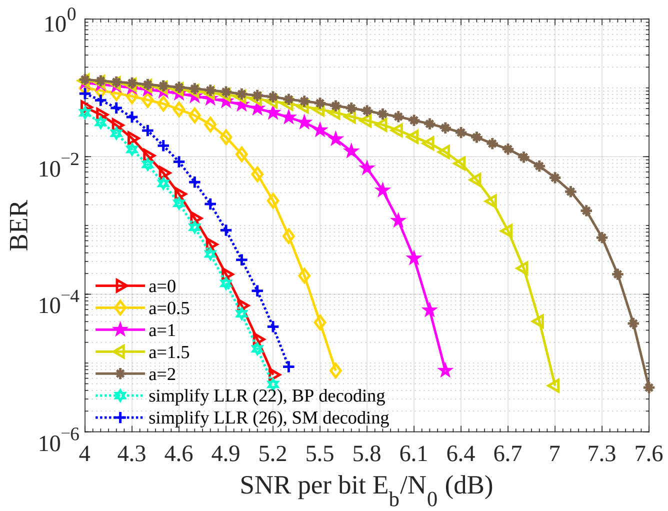

(**a**)

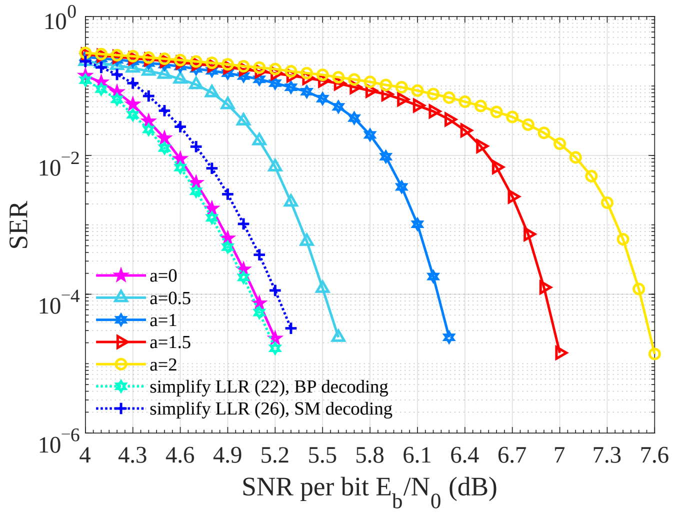

(**b**)

Figure 11. *Cont.*

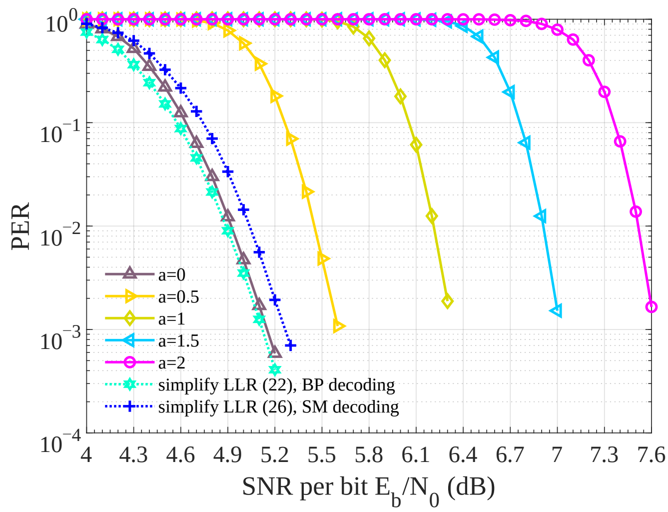

(**c**)

Figure 11. Detection performance for LDPC coded IEEE 802.15.4c MPSK signals under Rayleigh fading channel with $\Delta\sigma^2 = \alpha\sigma^2$, where $\rho = 1$. (**a**) BER performance; (**b**) SER performance; and (**c**) PER performance.

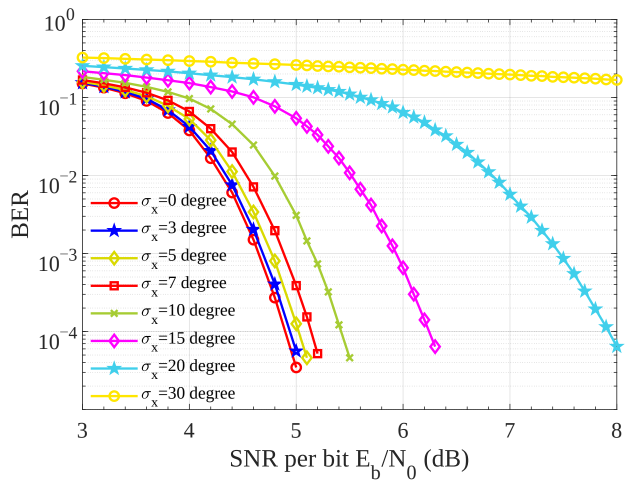

(**a**)

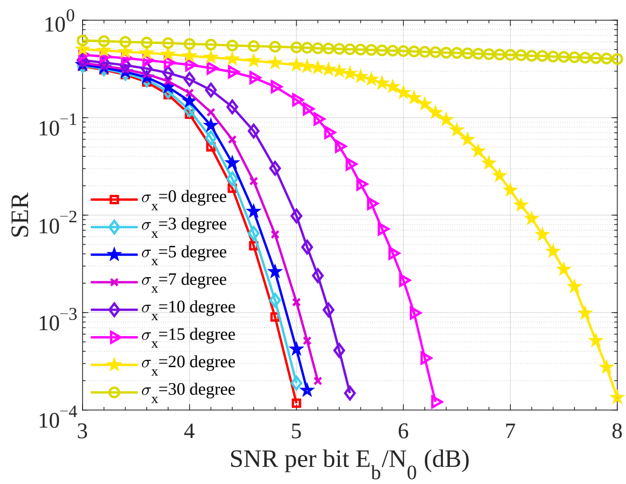

(**b**)

Figure 12. *Cont.*

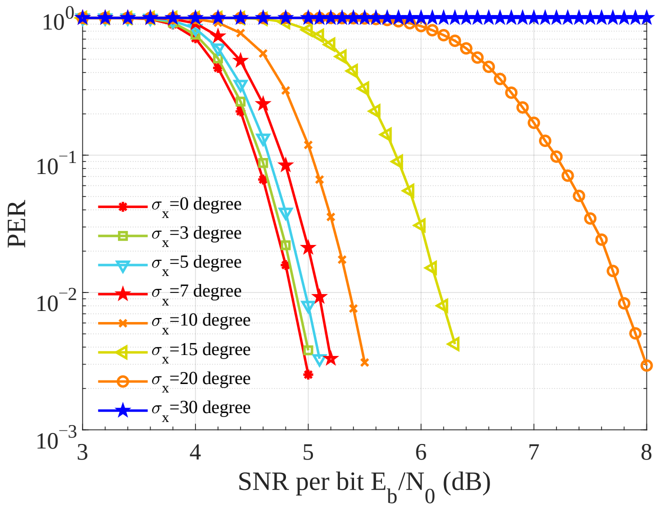

(**c**)

Figure 12. Detection performance for LDPC coded IEEE 802.15.4c MPSK signals under dynamic CPO channel, wherein LLR given in (8) is considered. BP algorithm is adopted for decoding, where $\rho = 1$. (**a**) BER performance; (**b**) SER performance; and (**c**) PER performance.

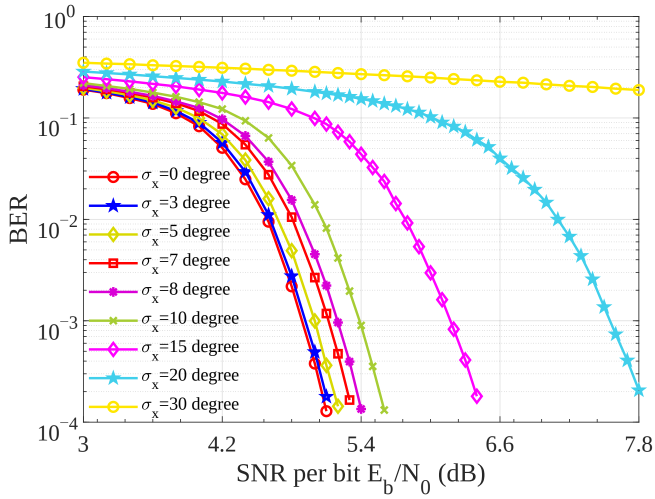

(**a**)

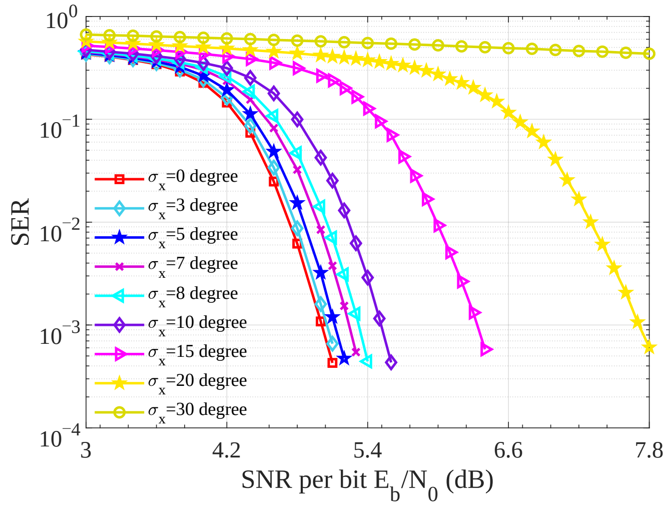

(**b**)

Figure 13. *Cont.*

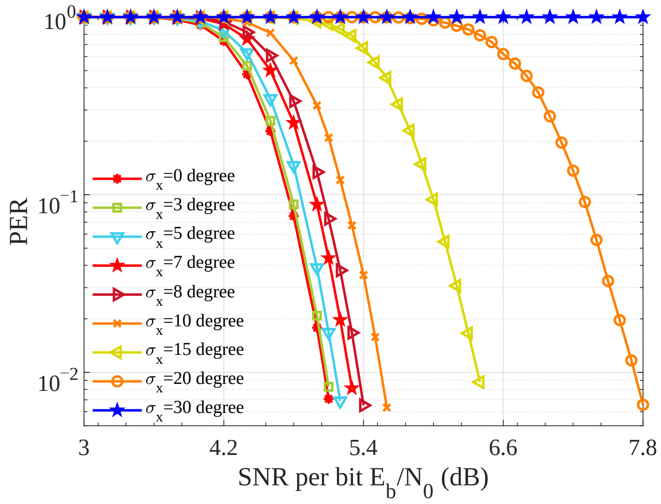

(**c**)

Figure 13. Detection performance for LDPC coded IEEE 802.15.4c MPSK signals under dynamic CPO channel, wherein LLR given in (16) is considered. MS algorithm is adopted for decoding, where $\rho = 1$. (**a**) BER performance; (**b**) SER performance; (**c**) PER performance.

5.6. Complexity Analysis

We compare the implementation complexity of various detection schemes, where $N = 1$. The structure block diagram of multiplication operation is shown in Figure 3 of [25]. Complex addition is the addition of two complex numbers. It is assumed that a comparison operation is equivalent to an addition operation. As shown in Table 3, compared with the exact LLR scheme, the simplified LLR scheme does not need CSI. Compared with the exact LLR given in (8) scheme, the simplified LLR proposed in (17) scheme does not need to calculate logarithmic function and Bessel function. As shown in Table 4, compared with the exact LLR scheme, the simplified LLR scheme does not require the exponential function. The multiplication/division operation of the exact LLR in (21) is 65.1 times the simplified LLR in (23); the addition/subtraction operation is 3 times the simplified LLR in (23); the modulus operation is 32 times the simplified LLR in (23). The conjugate operation is 16 times that of the simplified LLR in (23); the squaring operation is 80 times of the simplified LLR in (23). Obviously, compared with the exact LLR scheme, the complexity of our scheme is extremely reduced.

Table 3. Complexity comparation of the LLR calculation under the phase noncoherent channel.

Scheme	$(\bullet)(\bullet)$ or $(\bullet)/(\bullet)$	$(\bullet)\pm(\bullet)$	$\lvert\bullet\rvert$	$(\bullet)^*$	$(\bullet)^2$	$\ln(\bullet)$	$I_0(\bullet)$	CSI	$e^{(\bullet)}$	Re
(8)	1156	1016	64	1024	64	4	64	✓	\	\
(16)	1024	990	64	1024	8	\	\	\	\	\

Table 4. Complexity comparation of the LLR calculation under the Rayleigh fading channel.

Scheme	$(\bullet)(\bullet)$ or $(\bullet)/(\bullet)$	$(\bullet)\pm(\bullet)$	$\lvert\bullet\rvert$	$(\bullet)^*$	$(\bullet)^2$	$\ln(\bullet)$	$I_0(\bullet)$	CSI	$e^{(\bullet)}$	Re
(21)	4164	3000	2048	1024	5120	\	\	\	64	\
(23)	64	990	64	64	64	\	\	\	\	\

6. Conclusions and Future Work

This paper proposes two simple schemes to quickly generate bit LLR for coded MPSK signals: one for the phase noncoherent channel and the other for the Rayleigh fading channels. Our analysis shows that, when compared with the traditional optimal method, the scheme in this paper greatly reduces the implementation complexity. The proposed algorithm is applied to IEEE 802.15.4 WSNs to verify its effectiveness. The simulation results show that under both phase noncoherent and Rayleigh fading channels, the proposed simplified algorithm can depict an appropriate performance loss.

There are several directions remaining for future research. First, it is pointed out that we focus all our attention on end-to-end communication. The extension to distributed detection is straightforward and worthy of further study. Furthermore, all of the analysis is tailored uniquely for a slow changing channel, and the extension to more complex channel case, e.g., fast changing fading channel, is a challenging problem. In addition, only the CPO is considered to characterize the effect of the channel transmission; the channel with carrier frequency offset is also worthy of further study.

Author Contributions: Conceptualization, B.X. and G.Z.; methodology, G.Z. and C.H.; software, G.Z. and H.L.; validation, G.Z. and H.L.; formal analysis, H.L.; investigation, B.X. and G.Z.; resources, B.X.; data curation, H.L.; writing—original draft preparation, C.M. and H.L.; writing—review and editing, B.X. and G.Z.; visualization, C.M. and H.L.; supervision, B.X. and G.Z.; project administration, B.X.; and funding acquisition, G.Z. and C.H. All authors have read and agreed to the published version of the manuscript.

Funding: This research was funded by the National Natural Science Foundation of China grant numbers [61701172 and 41605122], the Henan Province Soft Science Research grant number [222400410440], the Key Laboratory of Middle Atmosphere and Global environment Observation grant number [LAGEO-2021-04], the backbone teacher training program of HAUST, the Natural Science Foundation of Henan Province grant number [162300410097], and the Scientific and Technological Innovation Team of Colleges and Universities in Henan Province grant number [20IRTSTHN018].

Institutional Review Board Statement: Not applicable.

Informed Consent Statement: Not applicable.

Data Availability Statement: Not applicable.

Acknowledgments: We thank the National Natural Science Foundation of China for the financial support.

Conflicts of Interest: The authors declare no conflicts of interest.

References

1. Walther, J.; Jong, C.D. Technology for More Effective Healthcare. *IEEE Multimed.* **2009**, *16*, 5–7. [CrossRef]
2. Torres, C.; Fried, J.C.; Rose, K.; Manjunath, B.S. A Multiview Multimodal System for Monitoring Patient Sleep. *IEEE Trans. Multimed.* **2018**, *20*, 3057–3068. [CrossRef]
3. Kirsal Ever, Y. Secure-Anonymous User Authentication Scheme for e-Healthcare Application Using Wireless Medical Sensor Networks. *IEEE Syst. J.* **2019**, *13*, 456–467. [CrossRef]
4. Muhammed, T.; Mehmood, R.; Albeshri, A.; Katib, I. UbeHealth: A Personalized Ubiquitous Cloud and Edge-Enabled Networked Healthcare System for Smart Cities. *IEEE Access* **2018**, *6*, 32258–32285. [CrossRef]
5. Alhussein, M.; Muhammad, G. Voice Pathology Detection Using Deep Learning on Mobile Healthcare Framework. *IEEE Access* **2018**, *6*, 41034–41041. [CrossRef]
6. Alemdar, H.; Ersoy, C. Wireless sensor networks for healthcare: A survey. *Comput. Netw.* **2010**, *54*, 2688–2710. [CrossRef]
7. Ramgopal, K. Applications of wireless sensor networks in healthcare. In *IoT and WSN Applications for Modern Agricultural Advancements: Emerging Research and Opportunities*; IGI Global: Hershey, PA, USA, 2020; pp. 8–40.
8. Djedouboum, A.C.; Abba Ari, A.A.; Gueroui, A.M.; Mohamadou, A.; Aliouat, Z. Big Data Collection in Large-Scale Wireless Sensor Networks. *Sensors* **2018**, *18*, 4474. [CrossRef] [PubMed]
9. Kumar, P.; Kumari, S.; Sharma, V.; Sangaiah, A.K.; Wei, J.; Li, X. A certificateless aggregate signature scheme for healthcare wireless sensor network. *Sustain. Comput. Inform. Syst.* **2018**, *18*, 80–89. [CrossRef]
10. Ayyildiz, C.; Erdem, H.E.; Dirikgil, T.; Dugenci, O.; Kocak, T.; Altun, F.; Gungor, V.C. Structure health monitoring using wireless sensor networks on structural elements. *Ad Hoc Netw.* **2019**, *82*, 68–76. [CrossRef]
11. Akyildiz, I.F.; Su, W.; Sankarasubramaniam, Y.; Cayirci, E. Wireless sensor networks: A survey. *Comput. Netw.* **2002**, *38*, 393–422. [CrossRef]
12. Ko, J.; Lu, C.; Srivastava, M.B.; Stankovic, J.A.; Terzis, A.; Welsh, M. Wireless Sensor Networks for Healthcare. *Proc. IEEE* **2010**, *98*, 1947–1960. [CrossRef]
13. Kumar, D.P.; Amgoth, T.; Annavarapu, C.S.R. Machine learning algorithms for wireless sensor networks: A survey. *Inf. Fusion* **2019**, *49*, 1–25. [CrossRef]

14. *IEEE 802.15.4-2015 Standard*; IEEE Standard for Low-Rate Wireless Networks. IEEE Press: New York, NY, USA, 2016.
15. *ISO/IEC/IEEE Standard 802.15.4-2018*; Information Technology-Telecommunications and Information Exchange between Systems-Local and Metropolitan Area Networks-Specific Requirements-Part 15-4: Wireless Medium Access Control (MAC) and Physical Layer (PHY) Specifications for Low-Rate Wireless Personal Area Networks (WPANs). IEEE Press: New York, NY, USA, 2018.
16. Li, Q.; Du, P.; Bi, G. Generalized soft decision metric generation for MPSK/MQAM without noise variance knowledge. In Proceedings of the 14th IEEE Proceedings on Personal, Indoor and Mobile Radio Communications (PIMRC 2003), Beijing, China, 7–10 September 2003; pp. 1027–1030.
17. Yuan, H.; Kam, P. The LLR Metric for q-ary LDPC Codes with MPSK Modulation over Rayleigh Channels with Imperfect CSI. *IEEE Trans. Commun.* **2012**, *60*,1793–1799. [CrossRef]
18. Cao, S.; Kam, P.-Y.; Yu, C. Pilot-Aided Log-Likelihood Ratio for LDPC Coded MPSK-OFDM Transmission. *IEEE Photonics Technol. Lett.* **2013**, *25*, 594–597. [CrossRef]
19. Jeon, H.J.; Demeechai, T.; Lee, W.G.; Kim, D.H.; Chang, T.G. IEEE 802.15.4 BPSK receiver architecture based on a new efficient detection scheme. *IEEE Trans. Signal Process.* **2016**, *58*, 4711–4719. [CrossRef]
20. Zhang, G.; Wen, H.; Wang, L.; Song, L.; Tang, J.; Liao, R. Simple and robust near-optimal single differential detection scheme for IEEE 802.15. 4 BPSK receivers. *IET Commun.* **2019**, *13*, 186–197. [CrossRef]
21. Zhang, G.; Wen, H.; Wang, L.; Zeng, X.; Tang, J.; Liao, R.; Song, L. Multiple symbol differential detection scheme for IEEE 802.15. 4 BPSK receivers. *IEICE Trans. Fundam. Electron. Commun. Comput. Sci.* **2018**, *101*, 1975–1979. [CrossRef]
22. Zhang, G.; Wen, H.; Wang, L.; Xie, P.; Song, L.; Tang, J.; Liao, R. Simple adaptive single differential coherence detection of BPSK signals in IEEE 802.15. 4 wireless sensor networks. *Sensors* **2018**, *18*, 52. [CrossRef]
23. Zhang, G.; Han, C.; Ji, B.; Shi, C.; Xie, P.; Yang, L. A new multiple-symbol differential detection strategy for error-floor elimination of IEEE 802.15.4 BPSK receivers impaired by carrier frequency offset. *Wirel. Commun. Mob. Comput.* **2019**, *2019*, 5409612. [CrossRef]
24. Zhang, G.; Wang, D.; Song, L.; Wu, H.; Xie, P.; Ji, B.; Wen, H. Simple non-coherent detection scheme for IEEE 802.15. 4 BPSK receivers. *Electron. Lett.* **2017**, *53*, 628–629. [CrossRef]
25. Park, D.; Park, C.S.; Lee, K. Simple design of detector in the presence of frequency offset for IEEE 802.15.4 LR-WPANs. *IEEE Trans. Circuits Syst. II Express Briefs* **2009**, *56*, 330–334. [CrossRef]
26. Zhang, G.; Shi, C.; Han, C.; Li, X.; Wang, D.; Rabie, K.; Kharel, R. Implementation-friendly and energy-efficient symbol-by-symbol detection scheme for IEEE 802.15. 4 O-QPSK receivers. *IEEE Access* **2020**, *8*, 158402–158415. [CrossRef]
27. Shi, C.; Zhang, G.; Li, H.; Han, C.; Tang, J.; Wen, H.; Wang, L.; Wang, D. Reduced-complexity multiple-symbol detection of O-QPSK signals in smart metering utility networks. *Electronics* **2020**, *9*, 2049. [CrossRef]
28. Divsalar, D.; Simon, M.K. Multiple-symbol differential detection of MPSK. *IEEE Trans. Commun.* **1990**, *38*, 300–308. [CrossRef]
29. Hagenauer, J.; Offer, E.; Papke, L. Iterative decoding of binary block and convolutional codes. *IEEE Trans. Inf. Theory* **1996**, *42*, 429–445. [CrossRef]
30. Motedayen-Aval, I.; Anastasopoulos, A. Polynomial-complexity noncoherent symbol-by-symbol detection with application to adaptive iterative decoding of turbo-like codes. *IEEE Trans. Commun.* **2003**, *51*, 197–207. [CrossRef]
31. Xi, D. *Bessel Function*; Higher Education Press: Beijing, China, 1998.
32. Van Tress, H.L.; Bell, K.L.; Zhi, T. Part I: Detection, Estimation and Filtering Theory. In *Detection Estimation and Modulation Theory*; Wiley: Hoboken, NJ, USA, 2012; pp. 1–176.
33. Lin, S.; Costello, D.J. *Error Control Coding: Fundamentals and Applications*; Prentise-Hall Publisher: Hemel Hempstead, UK, 1983; pp. 1–720.
34. ZZhang, G.; Wen, H.; Pu, J.; Tang, J. Build-in wiretap channel I with feedback and LDPC codes by soft decision decoding. *IET Commun.* **2017**, *11*, 1808–1814. [CrossRef]